



Giant ice rings in Southern Baikal: multi-satellite data help to study ice cover evolution and eddies under ice

Alexei V. Kouraev^{1,2}, Elena A. Zakharova^{3,4}, Andrey G. Kostianoy^{5,6}, Mikhail N. Shimaraev⁷, Lev V. Desinov⁸, Evgeny A. Petrov⁹, Nicholas M.J. Hall¹, Frédérique Rémy¹, Andrey Ya. Suknev¹⁰

5 ¹LEGOS, Université de Toulouse, CNES, CNRS, IRD, UPS Toulouse, France

²Tomsk State University, Tomsk, Russia

³EOLA, Toulouse, France

⁴Institute of Water Problems, Russian Academy of Sciences, Moscow, Russia

⁵P.P. Shirshov Institute of Oceanology, Russian Academy of Sciences, Moscow, Russia

10 ⁶S.Yu. Witte Moscow University, Moscow, Russia

⁷Limnological Institute, Siberian Branch of the Russian Academy of Sciences, Irkutsk, Russia

⁸Institute of Geography, Russian Academy of Sciences, Moscow, Russia

⁹Baikal Museum of the Irkutsk Scientific Center of the Russian Academy of Sciences, Listvyanka Village, Irkutsk Region, Russia

15 ¹⁰Great Baikal Trail (GBT) Buryatiya, Ulan-Ude, Russia

Correspondence to: Alexei V. Kouraev (alexei.kouraev@gmail.com)

Abstract. Ice cover on lakes is subject to atmospheric forcing from above and the influence of water dynamics and heat flux from below. One characteristic example of these influences in some large lakes, such as Lake Baikal in Russia, are the giant ice rings and the associated eddies under the ice cover. In April 2020 a giant ice ring appeared in Southern Baikal and a lens-like eddy was detected below the ice. We analysed the temporal evolution of ice cover using satellite images from multiple satellite missions - MODIS on Terra and Aqua, Sentinel-1 SAR, Sentinel 2 MSI, Landsat-8, PlanetScope, satellite photography from International Space Station, and radar altimetry data from Jason-3. Satellite imagery and meteorological data show an unusual temporal evolution of ice colour in April 2020, which was explained by water infiltration into the ice followed by the competing influences of cold air from above and the warm eddy below the ice. Tracking of ice floe displacement also makes it possible to estimate eddy currents and their influence on the upper water layer. Multi-satellite data contribute to a better understanding of the evolution of ice cover in the presence of eddies, role of eddies in horizontal and vertical heat and mass exchange and their impact on the chemistry and biology of the lakes and on human activity.



Introduction

Lakes can be viewed as an integrator of climate processes, and also strong indicator of climate change. This dual property stems from the way in which lakes respond to regional and global climate variation. Changing climatic or weather conditions affect the state and variability of natural parameters in lakes, such as temperature and salinity, stratification, currents, frontal zones, upwellings, eddies and gyres, ice and snow conditions, water level and biodiversity. Lakes are part of the Global Climate Observing System (GCOS) Essential Climate Variables (ECVs). The temperature, ice cover and water colour of 79 lakes are among the key parameters for the Global Terrestrial Network for Lakes (GTN-L).

Ice cover of lakes modulates heat and mass exchange between lake and atmosphere and affects physical, chemical and biological processes in the lakes. The state of the ice is also important for establishing transport on ice, for fishing activities and tourism. Ice cover is in constant evolution from its formation to a complete melting, due to the interaction between atmosphere (heat and wind forcing) from above and influence of water column (heat and water dynamics) from below. One characteristic example of such interaction in some large and deep lakes is the giant ice rings and the associated eddies under the ice cover.

Giant ice rings, most often observed in Lake Baikal, are a beautiful and not yet completely understood natural phenomenon. These are rings of dark ice with a typical diameter of 5-7 km; they appear on ice cover of some large lakes in a seemingly unpredictable manner from year to year. Ice is thinner and appears darker in the ring region, and in the center and outside the ring ice is thicker and looks white like the surrounding undisturbed ice cover (Granin et al., 2015, 2018; Kouraev et al., 2016, 2018, 2019). Due to their large size one of the best ways to observe and analyse them is from satellite imagery.

Giant ice rings were first observed in various places in Lake Baikal (Granin et al. 2005, 2008, Kouraev et al., 2016) but later we have found them in two other lakes - Hovsgol in Mongolia and Teletskoye in Altai, Russia. The total number of ice rings detected from satellite imagery is now close to 60 cases with the earliest documented ice rings in 1969 (Kouraev et al., 2019).

Ice rings have attracted the interest of both scientists and the general public, and several hypotheses have been put forward to explain the appearance of this strange phenomenon on the ice cover (see Kouraev et al., 2016 for the description). Today, the existing consensus is that ice rings are a surface manifestation (on the ice cover) of under ice heat fluxes produced by eddies, though the proposed mechanisms differ in terms of the type of the eddies.

In-situ observations of water structure beneath the ice rings in Southern (2009) and Middle (2013) Baikal (Granin et al., 2015, 2018) show the presence of an anticyclonic vortex; the authors explain the creation of this vortex by upwelling of deep

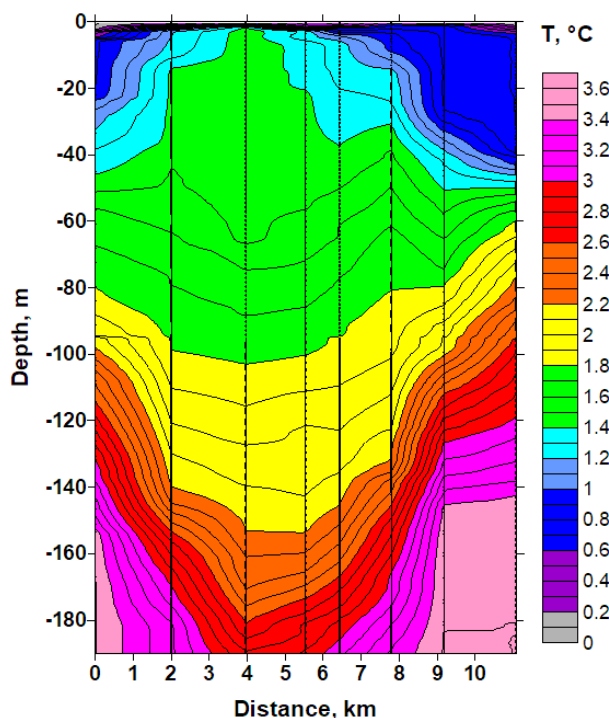


waters that can be associated with the rise of methane gas hydrates. The first clear physical explanation of this phenomenon
65 appeared after a comparison of satellite imagery of an ice ring with in-situ measurements of vertical structure of water
temperature and calculation of the density field (Kouraev et al., 2016). Our hydrographic surveys in the region of ice rings in
Lake Baikal (2012-2020) and in Lake Hovsgol (2015) have shown the presence of warm lens-like (double-convex form)
intrathermocline eddies beneath the ice cover (Kouraev et al., 2016, 2019), which are analogues of the most known Meddies
in the North Atlantic Ocean (Kostianoy and Belkin, 1989). CTD casts have shown that these eddies exist before and continue
70 to exist during ice ring appearance and development; they rotate in a clockwise (anticyclonic) direction and make a complete
rotation around its vertical axis in about 3 days.

Various in-situ measurements have shown that currents in the center of eddies are absent or weak. They are strongest at the
eddy boundary and it is here that increased heat exchange between ice and water lead to ice melting from below and the
75 formation of rings with thinner and darker ice, and not of circles (or round patches), as one may expect.

Analysis of thermal satellite imagery before the formation of an ice ring near Cape Nizhneye Izgolovye (Middle Baikal) in
2016 shows that the eddy was formed in ice-free conditions in late autumn 2015 by an outflow of water from the Barguzin
Bay. So in this case the main driver of eddy generation was the wind-induced movement of colder and lighter water (due to
80 specific temperature/density relationship for freshwater in the range from 0 to 4⁰C) in association with the coastline shape
(Kouraev et al., 2019). We suggest that this mechanism is typical for the eddies in this region and potentially for many other
eddies that eventually may generate ice rings.

A typical shape of an intrathermocline eddy in lake Baikal can be described as follows (Kouraev et al., 2019, see also Fig. 1).
85 It has a double-convex shape with a neutral layer located at about 45-50 m depth (depth of thermocline). The upper part
presents a dome-like rising of isotherms (and isopycnals), that displace laterally cold and well-mixed water that is typical for
neighbouring regions under the ice cover. The lower part of the eddy is bigger and deeper in extent than its upper part due to
a much weaker vertical stratification of temperature (and density) in this layer and presents a downward inclination of
isotherms (isopycnals) extending to depths of 200 m and more. While the ice ring size is comparable to the upper dome size,
90 the area affected by the eddy in the neutral layer is larger, reaching 10-12 km in diameter (Fig.1).



95 **Fig 1. Vertical section of water temperature (°C), 28-30 March 2018, across the eddy in the region of Cape Nizhneye Izgoloye (Middle Baikal). Vertical lines - station positions. This eddy led to the formation of a giant ice ring in late April 2018 (http://icerings.org/news_en.htm).**

In April 2020 another giant ice ring appeared in the Southern Baikal. Earlier in situ observations of water structure in this region done on 3-4 April 2020 by the researchers from the Limnological Institute in Irkutsk (Russia) revealed an anticyclonic eddy (Zyryanov et al., 2020). Interestingly, the distribution of temperature reveals not a «classical» anticyclonic oceanic eddy with a maximum of the orbital velocity on the sea surface, but an intrathermocline lens-like eddy with exactly the same structure as described above

100

While the exact mechanism of how this eddy was formed is not clear, in this paper we would like to address how the evolution of ice cover can provide new information on the eddy itself. To start with, this case presented a quite unusual development of an ice ring as seen from the satellite imagery (Figure 2). Typically once an ice rings appears it gets darker and well developed, and then the ice breaks up inside the ring (Kouraev et al., 2016), but there is no significant change in ice appearance outside the eddy nor sudden changes of the ice ring size. However in 2020 it was quite different. For most of April the satellite imagery showed a white surface with the ice ring present and not changing in size, then suddenly the ice turned very dark for a couple of days, and then the ice ring appeared again - but this time much bigger and with a sharp contrast between white and dark regions (Figure 2). So far we have not seen such case of temporal evolution so were

105

110 intrigued and puzzled.



115 **Figure 2. A sequence of Sentinel-2 images (red band, Level 2A - bottom-of-atmosphere reflectance with atmospheric correction) for Southern Baikal on 15, 20 and 23 April 2020. Colour scheme is the same for the three images. Ice ring that looks like fish eye is located in the westernmost part of Southern Baikal.**

Various available satellite imagery (Landsat, Sentinel etc) for the period of observation of this ice ring showed well the specific stages of ice ring evolution but still the gap in time made understanding elusive. Daily MODIS imagery was helpful but its low spatial resolution limited the analysis. When daily high-resolution PlanetScope satellite images were added to the
120 analysis, the pieces of puzzle fell into place.

In this paper we will first present the region of study. Then we will analyse ice cover evolution and metamorphism in the context of meteorological data, and what we currently know about ice ring eddies. And then we will demonstrate how multi-satellite imagery with high temporal frequency and high spatial resolution can monitor ice displacement and reveal the size
125 and impact of the underwater eddy.

1. Data used

1.1. Satellite imagery

For analysing day-to-day changes of ice cover on the large scale we have used MODIS imagery (Moderate Resolution Imaging Spectroradiometer, onboard Terra and Aqua satellites) that has 250 m spatial resolution in the visible range. Both
130 Terra and Aqua provide daily images covering the whole of Lake Baikal. More detailed analysis was done using high-resolution data from Landsat-8 and Sentinel-2 satellites. Landsat 8 OLI (Operational Land Imager) has 15 m spatial resolution in panchromatic and 30 m in the visible, near (NIR) and short-wave (SWIR) infrared ranges; the satellite has a 16-day repeat cycle. We have also used images from Landsat 8 TIRS (Thermal Infrared Sensor) instrument that has 100 m spatial resolution. Sentinel-2 MSI (Multi-Spectral Instrument) has 10 m spatial resolution in the visible and NIR, and 20 m in
135 SWIR ranges. A constellation of two satellites (Sentinel-2A and -2B) provides temporal resolution of 2-3 days for Lake Baikal. MODIS, Landsat-8 and Sentinel-2 have sun-synchronous orbits and they revisit each place at the same local time (local late morning over Lake Baikal). We also used radar images from Sentinel-1 SAR (Synthetic Aperture Radar) in Level



1 GRDH Interferometric Wide (IW) swath mode in VV and VH polarisations. These SAR images have spatial resolution 5
by 20 m and they were terrain corrected and processed with ESA SNAP software.

140

However the gaps in time for availability of high-resolution imagery and presence of cloud cover were still limiting to our
understanding - we were missing some key moments in the evolution of ice cover in April 2020. Significant advancement
was reached when we integrated PlanetScope imagery (Planet Team, 2017) into analysis. PlanetScope is a constellation of
approximately 130 cubesats that provides daily images in the visible and NIR range with 3 m spatial resolution. PlanetScope
145 scenes are also taken in late morning of local time. Depending on the date there are either some gaps for the region of study
or some areas are seen by different PlanetScope satellites with several minutes between scenes.

1.2. Space photography

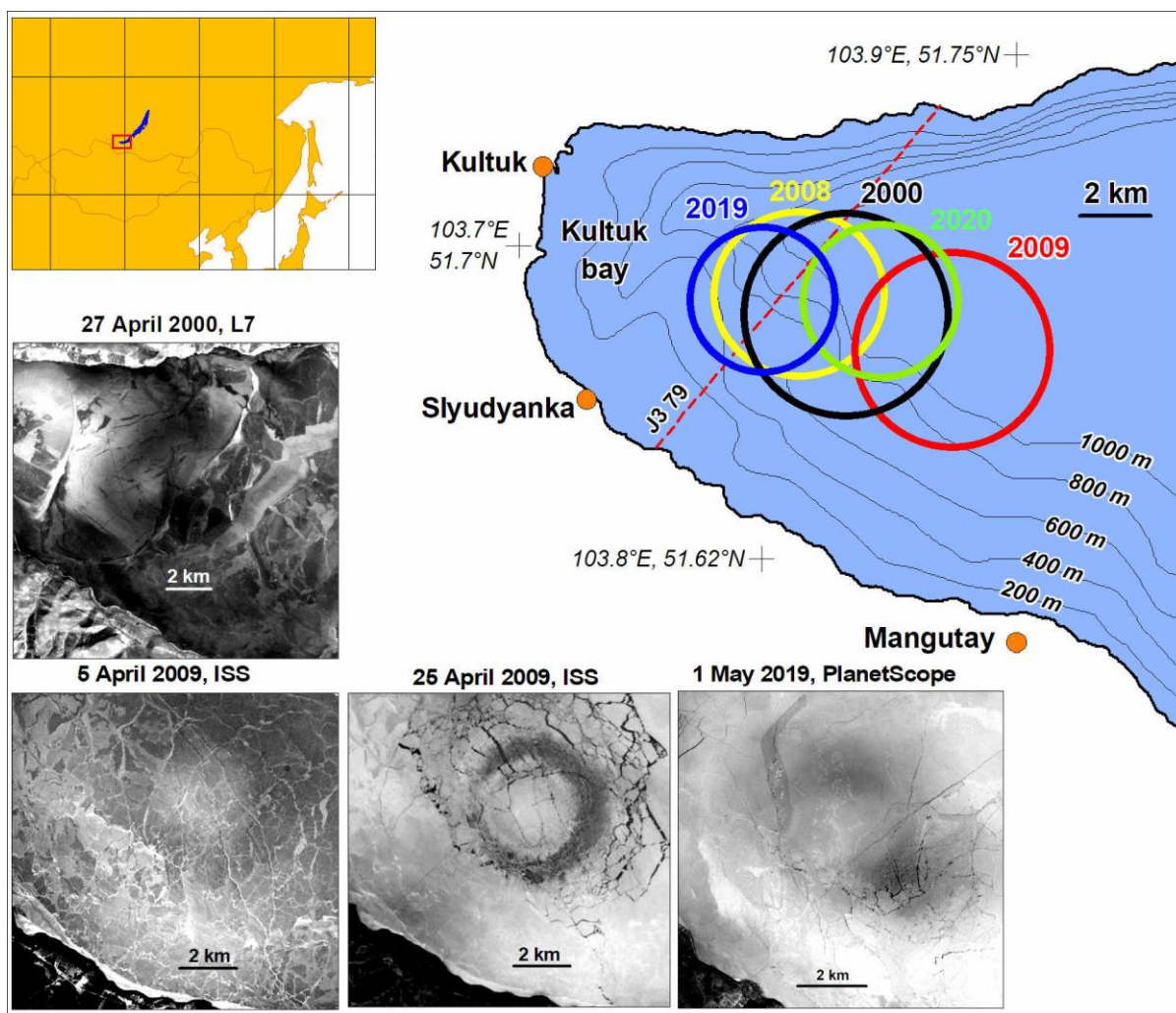
We have also analysed satellite photography from the International Space Station (ISS) from the space experiment "Uragan"
("Hurricane" in Russian) program. This program is the continuation of monitoring of Earth surface from orbital stations
150 initiated in 1976 and done first at the "Salyut" and then "Mir" stations (Evans et al., 2000). The "Uragan" program started on
1 January 2001 on the Russian orbital segment during the first expedition to the ISS, and is still ongoing. "Uragan" has 20-
30 tasks for monitoring natural processes, disasters and catastrophes. Cryospheric processes (glaciers, ice cover etc) are one
of the priorities, and monitoring of giant ice rings is one of the tasks. The high resolution photos of ice rings in 2009
presented on Figure 3 were taken on 5 April (32R3717, focal length 800 mm) and on 25 April (32R8494, focal length 300
155 mm) from the 400 km altitude. Unfortunately in April 2020 astronauts were not able to take photos of the ice ring due to the
acclimatisation regime after recent start of the mission.

1.3 Radar altimetry

Additional information was brought by satellite radar altimetry, which provides continuous and weather- and light-
independent observations along the tracks. While the main mission of radar altimeters is the monitoring of water level over
160 the ocean or large water bodies, the return signal also provides valuable information on the state of ice-covered or open
water surfaces. We have used data from the Jason-3 satellite, track 79 passing across Kultuk Bay (see Fig 1), cycles 141-157
(9 December 2019 - 16 May 2020) for the analysis. We used data from the nadir-looking radar altimeter operating in Ku
band (13.6 GHz), with the backscatter parameter processed with the Ice retracker. The backscatter coefficient is the ratio
between the power reflected from the surface and the incident power emitted by the onboard radar altimeter, expressed in
165 decibels (dB). Rough water surface typically has a low backscatter coefficient, while over ice cover it is high. The satellite
orbit is non sun-synchronous; repeat period is slightly less than 10 days along the same ground tracks; 20 Hz data provide an
along-track ground resolution of about 290 m.

2. Kultuk Bay and its ice rings

Southern Baikal - or to be more specific its extreme south-western part called Kultuk Bay - is one of the several regions in
170 Lake Baikal where ice rings are relatively common (Figure 3, see also statistics of ice rings in Kouraev et al., 2016). Two
other such places are Cape Krestovski and Cape Nizhneye Izgolovye in the Middle Baikal. Kultuk Bay is surrounded by
mountains on the northern and southern coast, and in the western part it communicates with a 190-km long Tunka Valley,
which is oriented mostly west-east. Strong and persistent wind from Tunka Valley affects most parts of Lake Baikal. All
around Lake Baikal people call this wind "Kultuk" in reference to its origins.



175

Figure 3. Overview map of the southern part of Lake Baikal with bathymetry and position of the giant ice rings in different years (coloured circles denote outer limits of ice rings) and some examples of ice rings from satellite imagery: 27 April 2000 (Landsat 7, band 4 near-infrared), 5 and 25 April 2009 – photography from ISS (red channel, georeferenced and reprojected), and 1 May 2019 (PlanetScope, near infrared band). Red dashed line marked "J3 79" - Jason-3 track No 79 over Lake Baikal. Projection: UTM Zone 48 North (WGS84).

180



The bottom of Kultuk Bay represents the western part of an abyssal plain with depth of more than 1500 m that occupies the main part of Southern Baikal. Near the coast this abyssal plain has boundaries with steep slopes. On the southern coast the inclination of these slopes is about 10° (isobath 1000 m is located at about 5.5 km from the coast); northern slopes are extremely steep - inclination 30-38° (in some cases 1000 m isobath is just 1.3 km away from the coast).

185 One may safely say that it is Kultuk Bay that made giant ice rings known worldwide. After a photo of an ice ring in 2009 (see Fig 3, image from 25 April 2009) taken by astronauts from the International Space Station was posted at NASA Earth Observatory web site ("Circles in thin ice", 2009) and then on other media sources, ice rings became an internationally known phenomenon. This spurred several scientific publications and initiated wider scientific research, including our own studies.

190

So far there are five documented cases of observations of ice rings on satellite images and space photography in Kultuk Bay (Figure 3, Table 1). Their average diameter is 4.7 km which is slightly smaller than many other ice rings in Lake Baikal (Kouraev et al., 2016, 2019) as the development of eddies is probably limited by the size and shape of Kultuk Bay. The duration of their manifestation on the ice cover was 15-17 days with the exception of 2009, when ice ring was visible one week longer. Last sighting of ice rings is just several days before ice break-up and melt, which is a typical feature for most ice rings detected in Lake Baikal. The earliest observation in Kultuk Bay was in 2000 and quite probably it is just limited by the amount of available satellite imagery before 2000; ice rings should exist earlier also. We have also discovered an as yet undocumented ice ring in May 2019 from Sentinel-2 imagery.

200 **Table 1. Inventory of ice rings and their characteristics in the Kultuk Bay. For the method used to define ice rings and the previous inventory see Kouraev et al. (2016, 2019).**

Year (end of winter)	Diameter, km	Lon E	Lat N	First seen ^a	Last seen ^a	Observation, days ^b	Open water date	Typical depth, m
2000	5.6	103.83	51.68	27/04	27/04	(1)		1000
2008	4.4	103.81	51.69	16/04 (1)	30/04 (3)	15	05/05	800
2009	5.2	103.88	51.67	04/04 (3)	27/04 (2)	24	05/05	1000
2019	4	103.80	51.69	15/04 (1)	01/05 (1)	17	04/05	600
2020	4.2	103.85	51.69	08/04 (2)	24/04 (1)	17	04/05	1000

^a Date format is (MM/DD); numbers in brackets - days since last ring-free scene for first ring seen, and days to first ring-free scene after last ring observation, ^b duration is defined as difference between the first observation and the last one. For observation in 2000 based on non-MODIS imagery, duration is put in brackets, meaning "at least X days)", though ring could have existed longer.

205

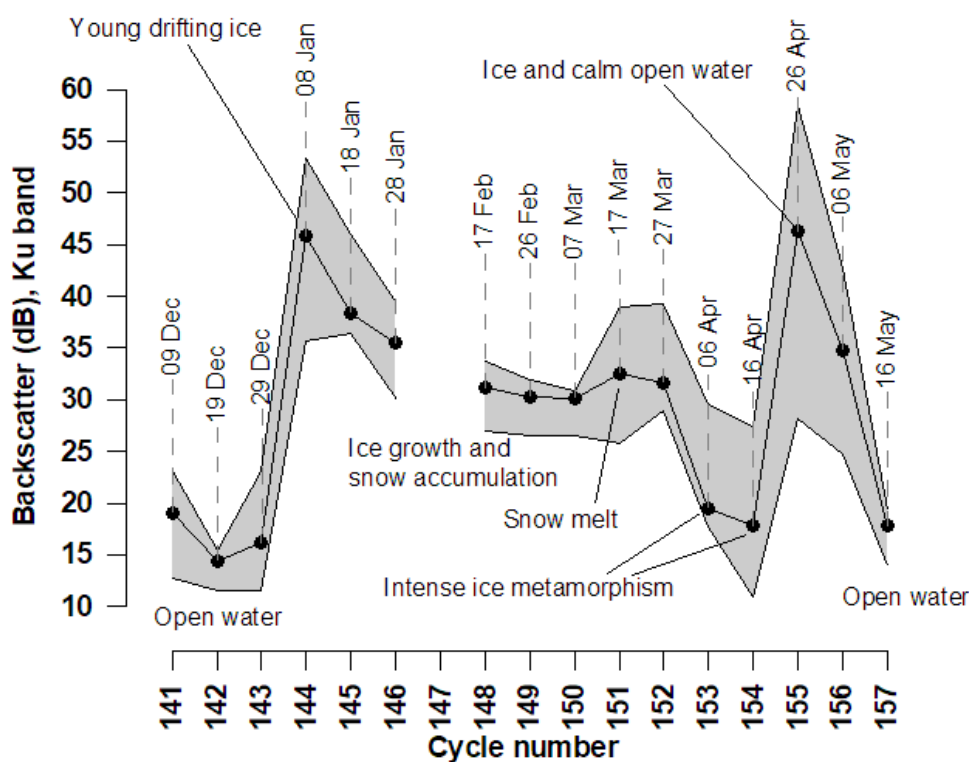
All these five rings were located on the southern slope of the abyssal plain, very close to one another, with the distance between their centers less than 5 km. In our previous work (Kouraev et al., 2016, 2019) we first suggested and then documented that lens-like eddies under ice may change their position, in some cases not even leading to the formation of ice



210 rings. We also suggested that while travelling, eddies may be trapped in head of abyssal plains, such as near Cape Nizhneye
Izgolovye. Kultuk Bay with similar bathymetry may be another such place where eddies are trapped.

3. Evolution of ice cover, giant ice ring and eddy in 2020

The combination of various multi-satellite imagery and data makes it possible to analyse in detail the evolution of ice cover
in Southern Baikal for winter 2020, with a focus on Kultuk Bay and the region of the giant ice ring observed in April 2020.
215 The first ice floes in Kultuk Bay appeared on 8-9 January and six days later the whole of Southern Baikal was frozen. The
evolution of the backscatter coefficient from the Jason-3 ground track shows that the appearance of young (nilas) drifting ice
led to a sharp 30 dB (from 15 to 45 dB) increase of backscatter (Fig. 4).



220 **Figure 4. Temporal evolution of Jason-3 backscatter coefficient (dB) in Ku band, track 97 in winter 2019/2020. Black line with dots - median values, grey zone - spread between maximum and minimum values.**

Until the end of March 2020 most of the southern part of the lake was snow-covered. A gradual decrease of Jason-3
backscatter down to 29-30 dB by the beginning of March indicates the process of snow accumulation, ice growth and
roughening. Snow disappearance by sublimation in the second half of March exposed a whitish surface of metamorphised
225 ice. This is seen on the visible images and also in slight (2-3 dB) increase of Jason-3 backscatter.

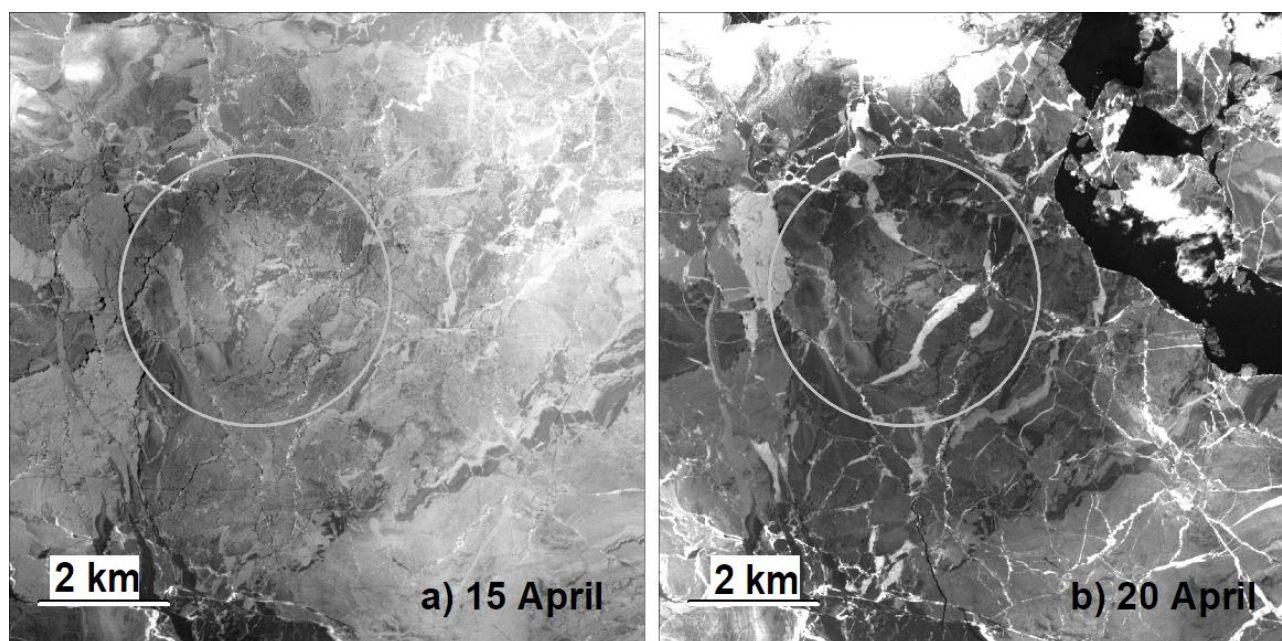


Snow had completely disappeared by 2 April, and on 8 April an ice ring was detectable for the first time. This giant ice ring had circular shape with outer diameter of 4.2 km and the width of the dark ring was 0.9 km (Fig 5a).

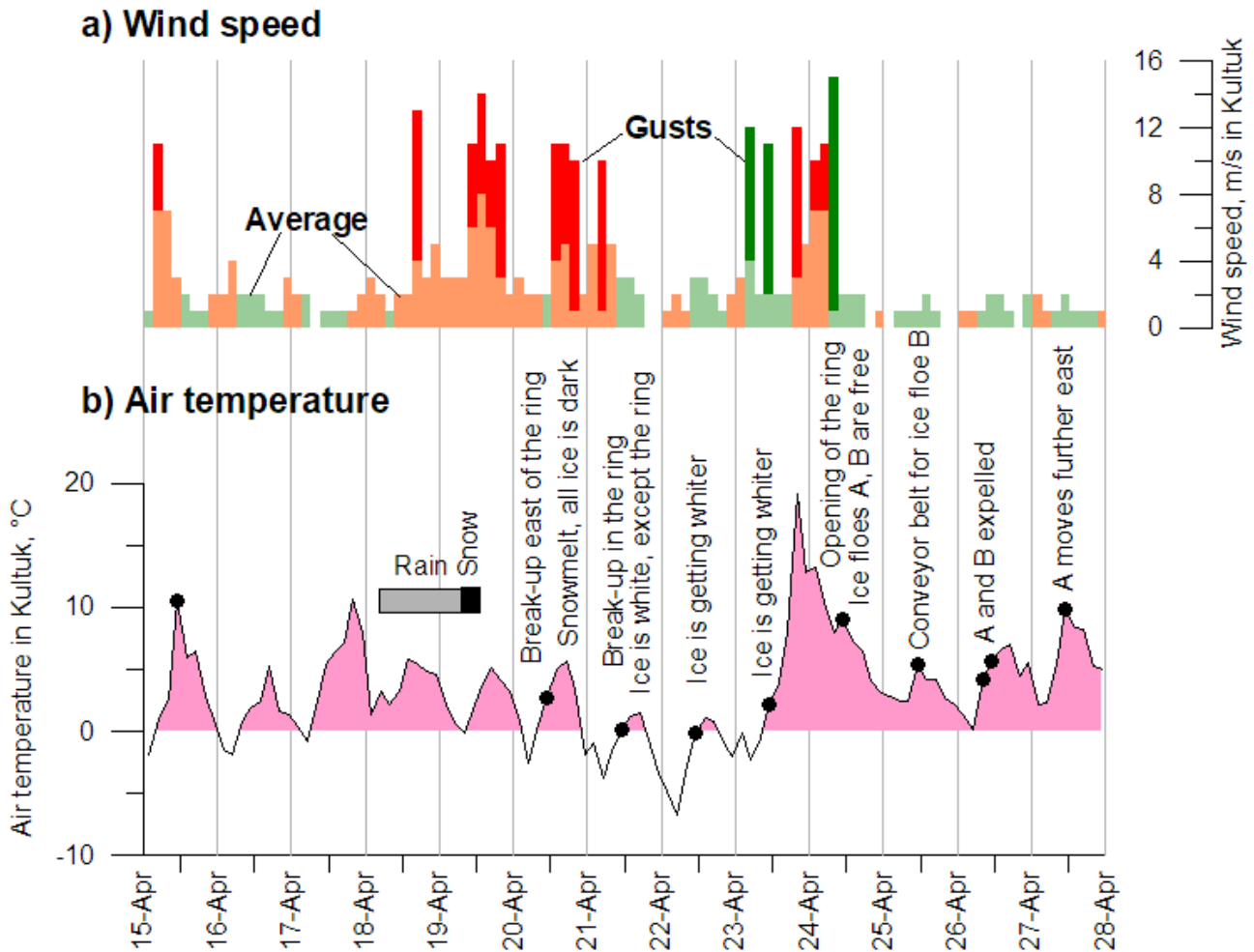
3.1. Ice break-up, displacement and metamorphism.

230 Ice cover in the southern part of Lake Baikal was stable until 18-19 April 2020 and afterwards influence of several meteorological factors – wind, air temperature and precipitation - started to affect the ice state.

Wind influence. According to data from the Kultuk meteorological station, starting from 18 April a constant Kultuk wind from the Tunka Valley was blowing with an average speed of 3-8 m/s and gusts up to 14 m/s (Fig 6). On 20 April wind
235 impact led first to ice break-up east of the ice ring region (Fig 5b). The next day under continuing westerly winds, the ice in the ring region itself was broken onto several ice floes (Fig 7a, 21 April 2020). A large ice floe "A" with a diameter of about 3 km corresponds to the initial center of the ice ring and eddy. As mentioned in the Introduction, this floe is thicker because eddy currents are weaker in the center of the eddy. During break-up this ice floe moved slightly to the north-west from its initial position. On 21-23 April wind was unstable and weak, so the position of the ice floes did not change much (Fig 7a-c),
240 except some slight compacting to the west between 21 and 22 April 2020.



245 **Figure 5. Evolution of ice cover in April 2020. a) 15 April and b) 20 April, Sentinel-2B, red band. Grey circle – outer limit of ice ring as defined from image on 15 April. All images are to scale. Color stretching is different for each image to enhance the contrast. Projection UTM 48N.**



250 Figure 6. Evolution of a) wind and b) air temperature for 15-28 April 2020 at the Kultuk meteorological station (Russian Hydrometeorological Service). Wind speed is coloured as a function of the general direction. Wind coming from the Tunka Valley (Kultuk wind) was classed as wind coming from the direction 292.5°(WNW, main direction of the opening of the valley) with a $\pm 45^\circ$ span: 247.5 to 337.5°, or wind between WSW and NNW. Kultuk wind is coloured in peach/red, winds from all other directions – in light/dark green. For each of the two directions we also present two different estimates of wind speed: average wind speed (lighter colour), and maximal gusts (darker colour). Black circles on the air temperature graph – date and time of satellite images discussed in the text.

255

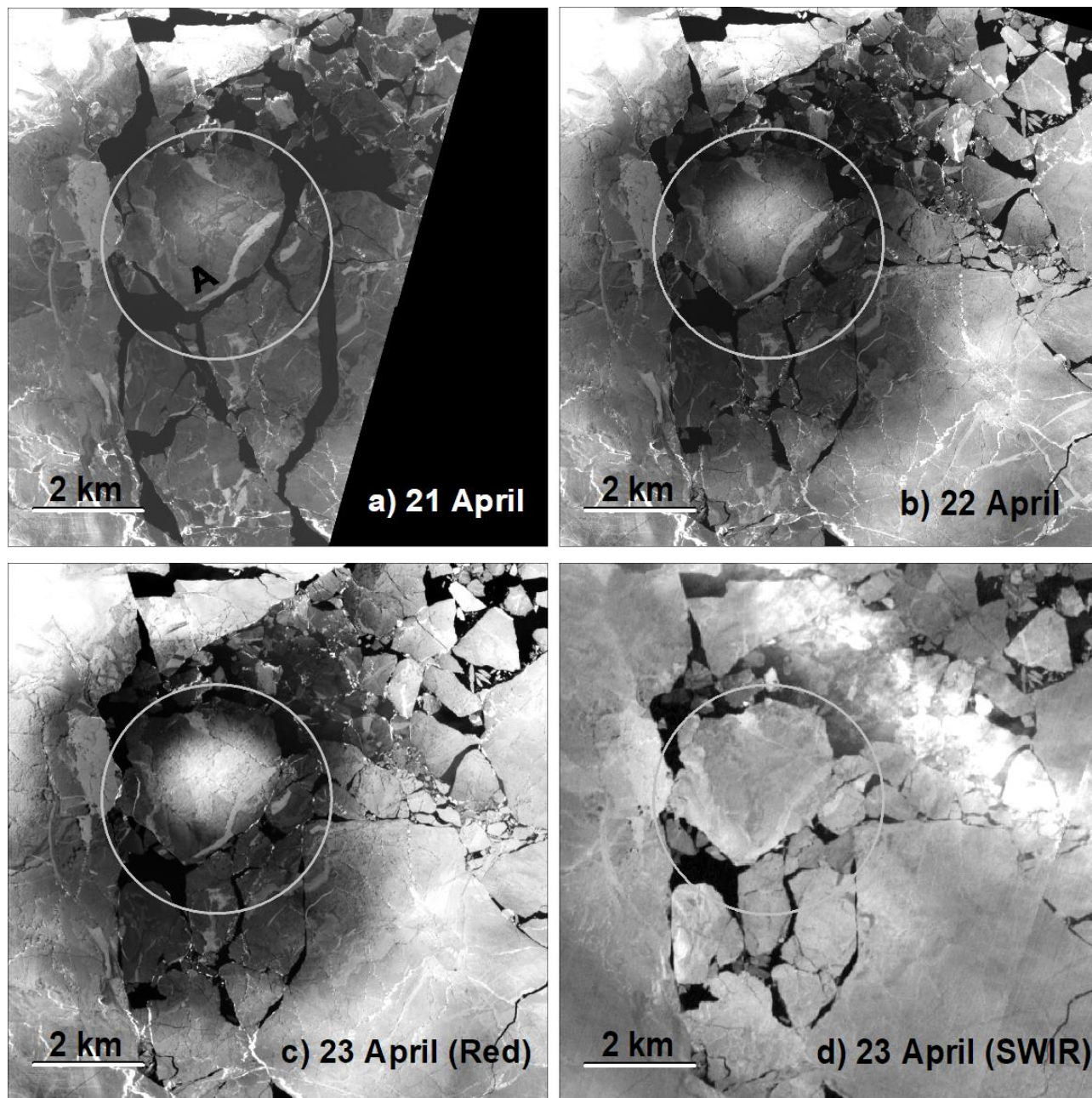


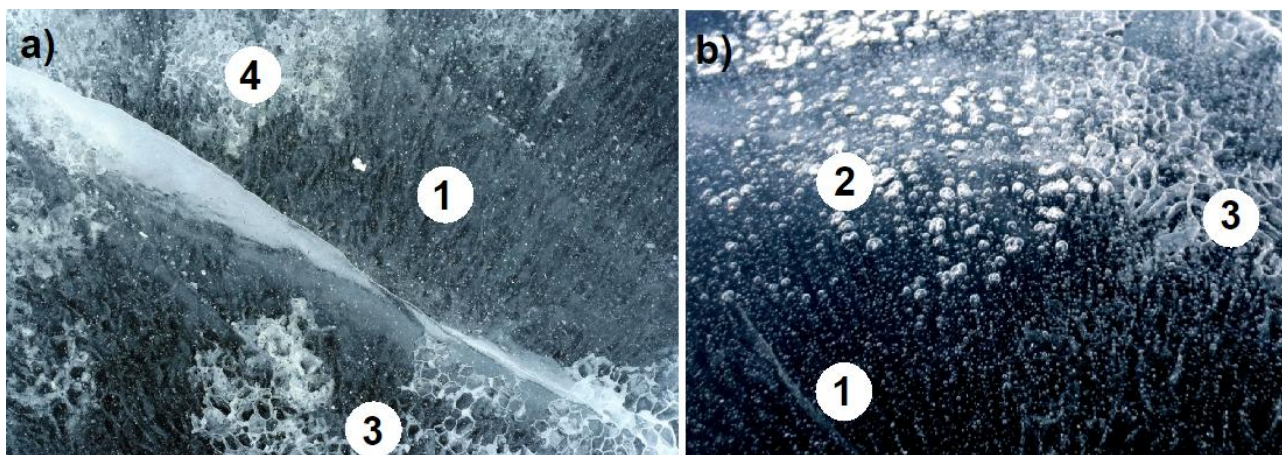
Figure 7. Same as Fig 5, but a) 21 April and b) 22 April - PlanetScope, red band, c) 23 April, Sentinel-2A, red band, d) same image as (c) but SWIR band. A – large ice floe mentioned in the text. Color stretching is different for each image to enhance the contrast.

260 **Ice metamorphism, warm air and precipitation.** From the beginning of April 2020 ice in Southern Baikal had already metamorphosed. Typically under intense solar radiation vertical crystals of columnar ice start to melt from the surface (Sokolnikov, 1959; Obolkina et al., 2000). This process is not specific to Lake Baikal, such metamorphisation is also seen in



many other lakes. Melting starts at the boundaries of the ice crystals, as the presence of impurities there decreases the melting point (Ashton, 2007). Ice metamorphism may take different forms, and some of them (Fig 8) can be vertical columns of tiny bubbles, large bubbles near the surface, or channels of air delineating boundaries of columnar ice crystals. Sometimes this process of formation of air channels is quite rapid and can be heard and observed with the naked eye (Kouraev et al., 2015). This metamorphism turns dark transparent crystalline ice into white ice and causes high reflectance well seen on satellite images in the visible and near-infrared ranges.

The described ice metamorphism changes the albedo, reducing the impact of solar radiation and delaying melting. It also significantly affects ice radiometric properties in the microwave range. The radar signal is very sensitive to the size and volume of scatterers in lake ice, especially air bubbles (Duguay et al., 2014) and we have previously documented large temporal change in the backscatter for ENVISAT/RA-2 and SARAL/AltiKa radar altimeters over the Middle Baikal (Kouraev et al., 2015). There is no Sentinel-SAR available for this period, but for Jason-3 observations ice metamorphism led to significant decrease of backscatter on 6 and 16 April (see Fig 4) - down to 15-20 dB. These values are almost comparable with rough open water conditions.



280 **Figure 8. Different manifestations of ice metamorphism on the ice cover surface. a) Southern Baikal, 10 April 2006 (Photo: E. Petrov) b) Middle Baikal, 3 April 2014 (Photo A. Kouraev). 1 - vertical lines of air bubbles; 2 - large bubbles just below ice surface; 3 - air channels showing limits of columnar ice crystals; horizontal size of these crystals is about 2-4 cm; 4 - similar to 3, but upper central parts of columnar ice is also white. Horizontal size for columnar crystals seen on (3) is about 2-4 cm.**

High values of air temperature of up to +10°C and more during the day and close to 0°C at night were prevalent during six consecutive days from 15 to 20 April 2020 (Fig 6b). At 5 h (local time) in the morning on 18 April light rain showers started and persisted until 8 h 19 April, and then were followed by light snow showers until 14 h on 19 April (also marked on Fig 6b). The air temperature was positive (up to 5.1°C) during the day and even at night just briefly decreased down to -2.6°C, so rain and snow created a liquid water layer on ice surface. Apparently all this water infiltrated the ice surface, filling the



290 cavities that were previously giving whitish aspect to the ice. As a result the ice surface turned very dark and extremely low
reflectance was observed on MODIS (Terra and Aqua), Sentinel-2 (Fig 2) and PlanetScope images on 19 and 20 April 2020
over a large area of Southern Baikal.

Cold event reveals the eddy. After another warm day on 20 April 2020, night temperatures plunged down to negative
values (down to -3.8°C) for the whole night of 20-21 April. As a result starting from 21 April satellite images became very
295 contrasty – there is still very dark ice in the region initially affected by the ring, but ice in the center of ice floe A and
elsewhere outside ice ring region is very white. This tendency further increased over the next two days. After a cold night
21-22 April (down to -6.7°C) a large area covering most of Southern Baikal became whiter. The white area of the ice floe A
got larger and the dark area in the ring region got smaller. The day of 22 April was cold (maximal values 1.1°C) as was the
following night (minimal values -2.3°C). Consequently, there was a stark contrast between white ice in the center of ice floe
300 A and in the outside regions, and a dark ice area located in and directly outside the ring region (see Figs. 2 and 7).

The situation on 23 April 2020 was recorded by images from MODIS sensors, Sentinel-2, PlanetScope and also Russian
Canopus-B ("Remote sensing..", 2020) satellites. In some cases these images were taken by journalists as evidence of a giant
methane bubble trapped under ice and just waiting to explode ("Giant gaz bubble..", 2020).

305 However we now have a more realistic explanation of these puzzling images. We have seen that warm weather and rain and
snow eliminated the surface manifestation of earlier ice metamorphism and led to very dark aspect of ice on 19-20 April
2020. This is equivalent to preparing a clean canvas for drawing a new picture. And then two painters - or two contradictory
forces acting on ice - cold air from above and warm eddy from below - started to paint a new picture on the ice.

310 Negative temperature likely led to the formation of a thin crust on the ice surface, turning it whitish again. This is seen on
images 21-23 April 2020 and is not limited to the eddy region but affects a much larger area in Southern Baikal (see also Fig.
2). Below the ice, eddy influence counteracts the impact of cold air, delaying or cancelling formation of a white crust. In
regions where the eddy current is stronger (eddy periphery) and where the ice is thin or broken, we continue to see dark ice
315 (Fig 7, a-c). This is further confirmed by comparing the Sentinel-2 images for 23 April in different bands. Contrast between
a white center and dark ring region was observed in three visible bands and one near-infrared band of MSI sensor, but not at
all in SWIR (Fig 7d). The SWIR band with its longer wavelength is better than other bands for seeing thin clouds, such as
the condensation trail from an airplane in the upper right corner on Fig. 7d. It is also less affected by reflection from small-
scale surface phenomena, such as ice crust, some types of snow etc. As a result we clearly see the distribution of ice floes
320 and fields with different signatures, but no ice ring.



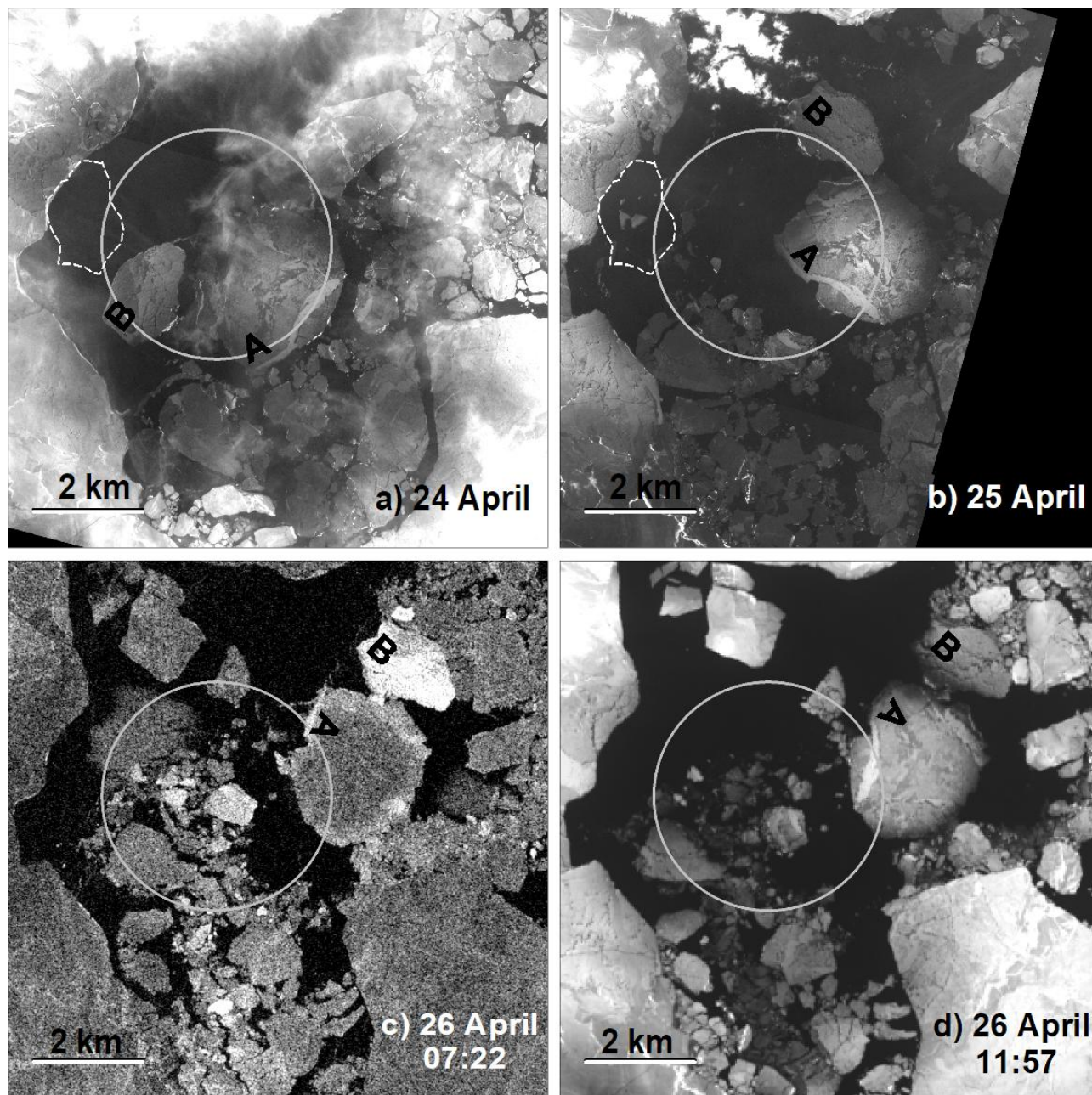
3.2. Ice tracking as a mean to assess eddy currents.

During our study of evolution of ice cover and metamorphism we collected various satellite imagery, sometimes with several images per day, for Kultuk Bay in April 2020. This brought a possibility to assess of eddy influence through the analysis of ice floe movement. In the early morning of 24 April a Kultuk wind with gusts of up to 11 m/s led to the displacement of ice floes 1.5-2.5 km to the south-east and the opening of the most of the area affected by the eddy. Starting from this time, the displacement of ice floes provides a unique opportunity to monitor and quantify the influence of the eddy by looking at ice floes A (discussed earlier) and B (Fig 9).

An elongated ice floe B with size of 2 km by 1.5 km was detached from the ice field west of the ice ring. Under the influence of Kultuk wind between 23 and 24 April 2020 it was displaced to the region of the eddy's outer boundary, where as we know current speeds are the greatest. Then, like a suitcase thrown onto a conveyor belt at the airport, this ice floe was rapidly transported along the eddy boundary. The image from 25 April (Fig 9b) shows that over one day ice floe B was transported for about 6 km (average speed 7 cm/s) almost without changing its orientation with respect to the eddy. Two lines of smaller pieces of broken ice floes follow the trail of ice floe B (Fig 9b) indicating curvilinear direction along the eddy boundary. Then on 26 April when it met an obstacle (ice floe A), ice floe B was expelled a further 2.3 km to the east, out of the eddy region (Fig 9 c,d). As the eddy no longer affected this ice floe, this time displacement happened without changing orientation to the North.

Ice floe A was located inside the eddy and its various parts were affected differently by eddy currents. As a result this ice floe manifested not so much lateral displacement as clockwise spinning. A presence of a thin and 2.3 km-long fish-shaped band of white ice on the surface of ice floe A helps to analyse this rotation.

A sequence of images for 24-26 April 2020 (Fig 9) and PlanetScope image for 27 April (not shown) help to define the positions of ice floes A and B at different dates (Fig 10) and estimate their rotation (Table 2). Ice floe B, while inside the eddy, was rotated 97° clockwise between 24 and 25 April. Ice floe A experienced strong clockwise motion between 24 and 27 April, with a total rotation of 219°. The rotational speed of ice floe A decreased when it left the eddy region, but still continued, likely due to the to spinning momentum. This was not the case for the ice floe B which was on the periphery of the eddy.



350

Figure 9. Same as Fig. 7, but f) 24 April and b) 25 April 2020, PlanetScope, red band, c) 26 April 2020, Sentinel-1B SAR, VV polarisation, d) 26 April 2020, Landsat-8, red band. A and B – large ice floes mentioned in the text, dotted line on (a) and (b) – position of ice floe B on the 23 April 2020. All time for satellite images is local time (GMT+8). Color stretching is different for each image to enhance the contrast.

355

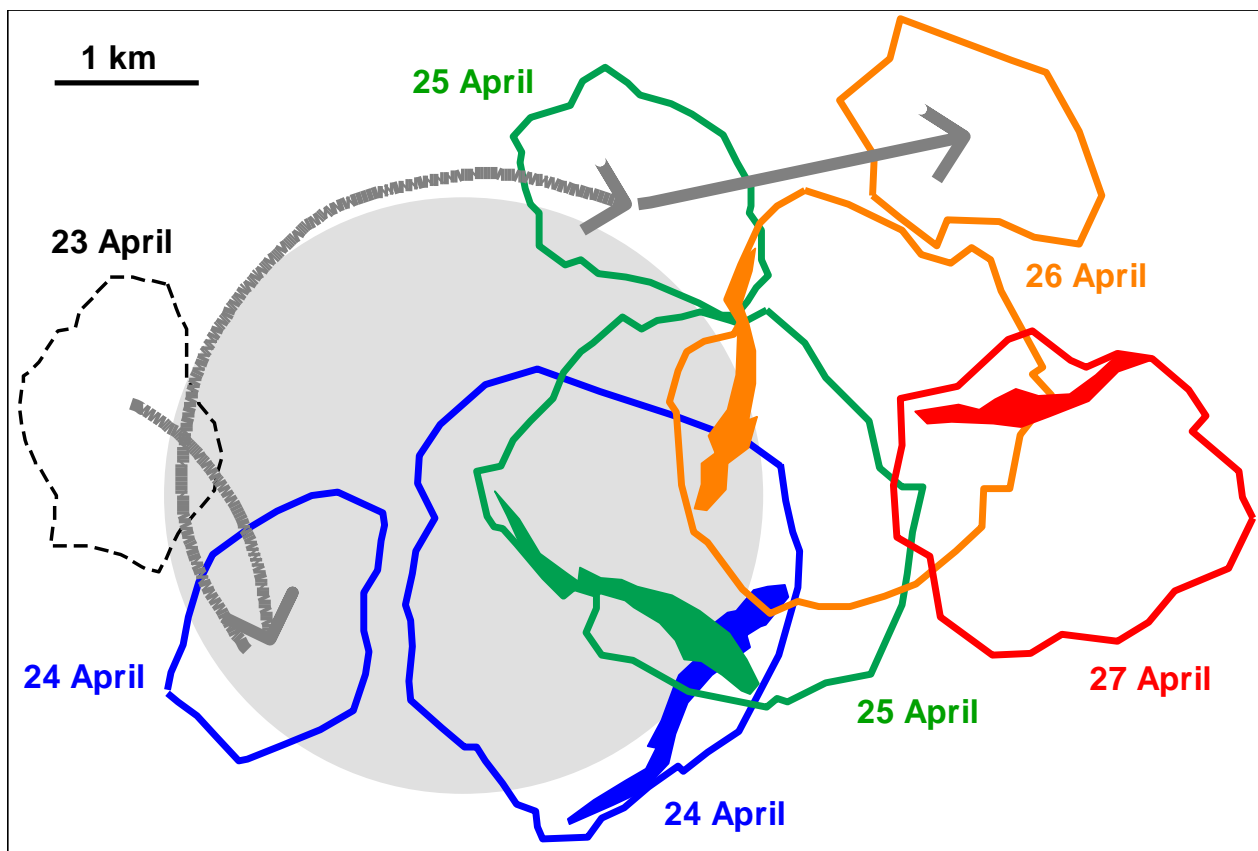


Figure 10. Schematic representation of position and displacement of ice floes A and B between 23 and 27 April 2020. Grey circle – approximate area affected by eddy, defined from ice ring outer limit on 15 April 2020.

360 Table 2. Angle and angular speed of ice floes A and B

Date and local time	Satellite	Angle of ice floe A (deg)	Angular speed (deg/hr)	Angle of ice floe B (deg)	Angular speed (deg/hr)
24 April 11:42	PlanetScope	0		0	
25 April 11:47	PlanetScope	84	3.49	97	4.02
26 April 07:22	Sentinel-1	150	3.37		
26 April 11:57	Landsat-8	156	1.31		
27 April 11:17	PlanetScope	219	2.70		
		Total: 219	Average: 3.05		

Discussions and conclusions

Imagery from multi-satellite missions, meteorological data and knowledge of water dynamics under ice, all taken together enhances the scope of analysis of the development of a giant ice ring and eddy in April 2020 in the Kultuk Bay, Lake Baikal.



365

"Redrawing" of the ice ring. Temporal analysis of ice metamorphism and evolution helps to understand and interpret the interplay between two influences – one from above (wind, sun radiation, air temperature, snow and rain) and one from below (warm eddy, currents). We have seen that the ice reflectance on satellite images changes from white (metamorphised) to completely dark and then to a very contrasting pattern around the eddy. This was caused first by water infiltration into the ice and then by the competing influences of cold air from above and warm water from below the ice, supplied by subsurface lens-like eddy.

370

It is interesting to note that after 20 April 2020 the dark area became larger (7.2 km diameter) than the initial ice ring (4.2 km diameter), although its center did not change much. As ice floe A moved NW from its initial position between 20 and 21 April, and numerous ice floes in the ring region slightly compacted westwards between 21 and 22 April, this creates the impression that the dark region has an elliptical form.

375

The conveyor belt. Tracking of ice floe displacement also makes it possible to estimate eddy currents and their influence on the upper water layer. We have seen how the eddy transports and expels ice floe B and how it spins ice floe A. This is in agreement with what we know about the spatial distribution of currents in the eddies under ice cover in Lake Baikal (Kouraev et al., 2016, 2019).

380

Estimation of rotational speed (Table 2) gives an average value of 3.05 °/hr (equivalent to a full rotation in 4.9 days) for ice floe A and 4.02°/day (full rotation in 3.73 days) for ice floe B. Our estimations of rotational speed for a similar eddy observed in 2016 near Cape Nizhneye Izgolovye in the Middle Baikal (Kouraev et al., 2019) from direct (current loggers) and indirect (temperature loggers) observations indicate a full rotation every 3 days. Rotation speed from ice floes A and B appear close to these values, given that there will inevitably be differences due to the duration of the effect, frictional losses, drag coefficient, wind forcing, etc.

385

The situation observed in April 2020 in Kultuk Bay is a relatively rare case, when during ice break-up ice rings don't just develop and then disappear (as was the case in 2009 and 2016 for Cape Nizhneye Izgolovye). In this case large-scale ice break-up allows us to observe how the eddy is transporting and rotating ice floes. There are several factors that made such observation possible. Kultuk Bay is a relatively narrow region and ice drift is limited in large-scale displacement, constraining the movement to west-east. Rapid ice deterioration due to thermal melt and limited large-scale wind-driven ice drift also facilitated observation of the eddy's influence on ice transport.

390

395

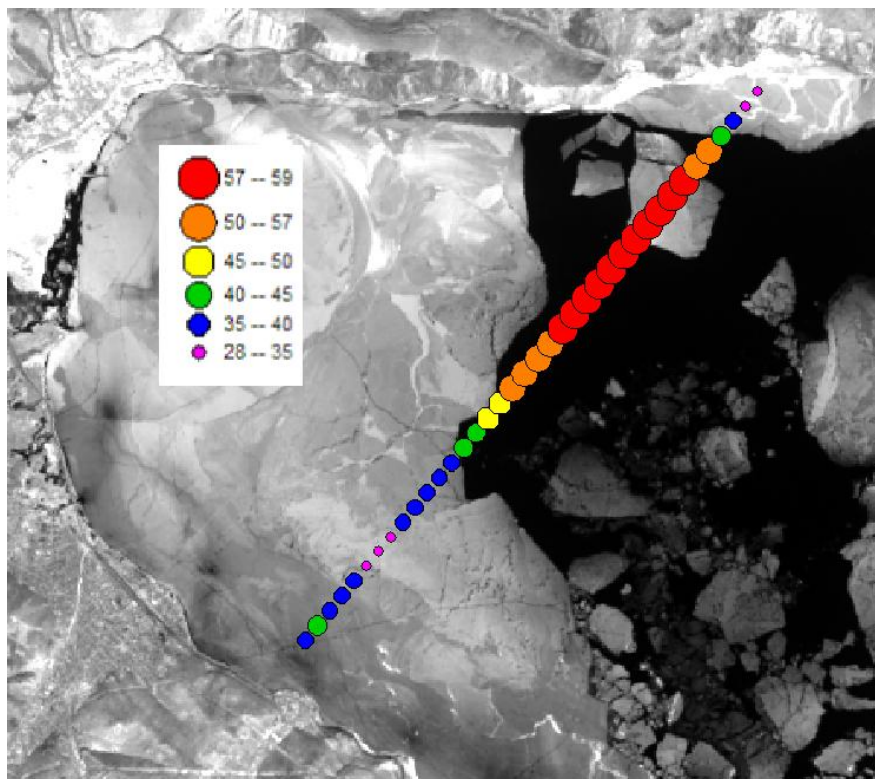
The power of multi-satellite imagery. There are still a lot of unknowns in the interpretation of ice cover state from visible, NIR, SWIR, TIR and microwave satellite images and data. When studying natural phenomena a complimentary data



approach is advantageous and it helps to use all existing sources of satellite imagery that may reveal some key elements in
400 ice cover development.

While for our case daily or sub-daily frequency of available satellite imagery was sufficient for analysing most of the
interesting features, if necessary ice floe tracking can be done on a much shorter time interval. For example, the time interval
between subsequent PlanetScope satellites is 90 seconds and this makes it possible to estimate the speed of relatively fast-
405 moving objects, such as river ice (Kääb et al., 2019). In some cases the same area can be covered by non-subsequent tracks
making this time lag larger to track slower moving objects.

Satellite radar altimetry provides useful information on the state of ice cover and of water surface. On 26 April 2020 ice
break-up led to the appearance of large areas of open water protected from the wind by drifting ice fields. This calm water
410 acted like a mirror and brought specular reflection and increased Jason-3 backscatter up to 58 dB (Fig 11). Actually the
backscatter may have been even higher but was cut out by the ice retracker algorithm at 58 dB. The detached ice floe
presented in the northern part of the track on Fig 11 apparently drifted away between 11h 30 min (time of Landsat image)
and 20 h (time of Jason-3 observation). The consolidated ice edge remained the same and is resolved by Jason-3 data with
high spatial accuracy (290 m). This ability of radar altimetry missions for robust discrimination between open water and ice
415 was noted in our work for T/P-Jason, GFO and ENVISAT-AliKa series over various Eurasian lakes and rivers (Kouraev et
al., 2007; 2008; 2015; Zakharova et al., 2021). However one may also note the spatial variability of backscatter over fast ice,
such as the decrease of signal over a white (potentially rough and hummocked) ice field (Fig 11, violet dots). This shows the
possibility for further ice type classification from radar altimetry data, based on field measurements along satellite tracks and
quasi-simultaneous with satellite overpasses.



420

Figure 11. Backscatter values (dB) for the Jason-3 track 79, cycle 155 (26 April 2020, 20 h local time) overlaid over Landsat-8 image for 26 April 2020, 11h30 local time.

Another crucial source of information to assess the interaction of eddies under ice and ice cover itself is thermal infrared imagery. The Landsat 8 TIR image for 26 April 2020 (not shown) reveals water with warm 3.1-3.6°C temperature in the leads (open water) near the northern coast due to the effect of sun reflection of south-oriented mountain slopes on the coast. For the region of the eddy water temperature was 2.4-2.6°C and the thermal contrast was not enough to detect the eddy.

However there are cases when thermal imagery may clearly reveal the difference in surface temperature due to an underwater eddy, as in winter 2018 near Cape Nizhneye Izgolovye (Fig 12). During our field work on 13-18 February 2018 we took vertical profiles of temperature and identified another lens-like eddy, similar to the ones typical to this region. The thermal image from Landsat 8 on 6 March 2018 clearly shows that increased temperature and heat exchange between the upper dome of the eddy and the ice led to spatial differences in ice surface temperature. Despite the ice being 60-70 cm thick at the time, the eddy created a circular zone more than 2°C warmer than the surrounding regions. The eddy did not move during the second field work period in late March, and an ice ring was formed there in April 2018.

435

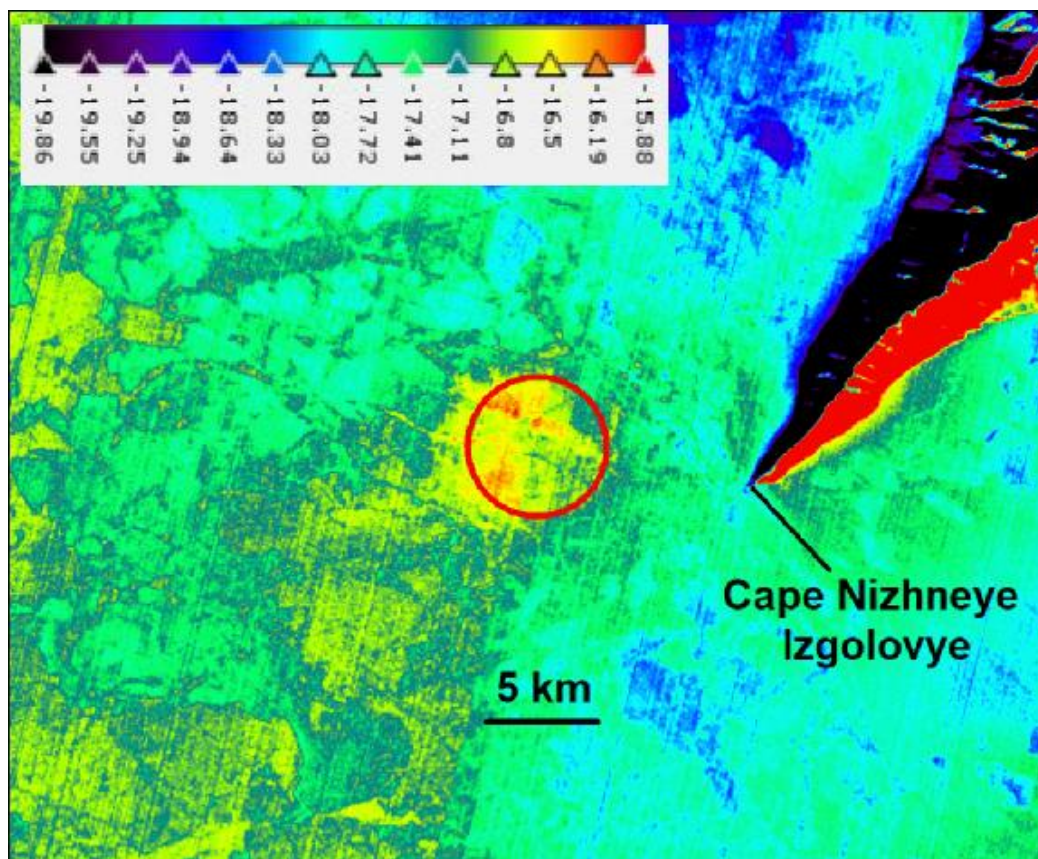


Figure 12. Surface temperature (°C) from Landsat 8 image on 6 March 2018. Red circle - position of outer eddy limit as defined from in situ data in February 2018.

440 **Monitoring eddies.** Intrathermocline lens-like eddies are a special type of oceanic eddy. They have been observed in various regions of the World Ocean, but have only recently been discovered in lakes (Kouraev et al., 2016, 2019). While lens-like eddies have a variety of generation mechanisms (Kostianoy and Belkin, 1989), the physics and hydrodynamics of lens-like eddies in lakes and in the ocean are strikingly similar.

445 As ice cover is much thinner and weaker in the regions of eddies, the presence of eddies under the ice and the formation of giant ice rings is a clear danger for people travelling on ice in lakes such as Baikal or Hovsgol (Kouraev et al. 2016, 2019). Better understanding of the interaction between eddies and ice, the evolution of ice cover in the presence of eddies, timely detection; monitoring and potentially forecast of ice rings or regions of weakened ice, is a major concern for safety on lake ice.

450 We expect the investigation of the 3-D structure and internal water dynamics of lens-like eddies in lakes to contribute to understanding the same lens-like eddies in the World Ocean. Of particular interest could be study of the eddies in the Arctic



Ocean. These eddies are smaller than typical oceanic eddies (Kostianoy, Belkin, 1989) - about 10 km wide - and thus more difficult to detect and explore. In cases when such eddies interact with sea ice surface, they may create ice rings or similar deformations in ice structure and can be possibly detected from satellites. The methodology of eddy studies from lake ice
455 may be applied to these eddies.

Investigations of lens-like eddies in the ocean is complicated by the fact that their detection is fortuitous, requires research vessels, deep CTD stations, etc. Field studies of eddies in ice-covered lakes are greatly facilitated by the presence of stable ice cover. CTD casts from the ice give a unique opportunity to make measurements with a fine spatial resolution of several
460 hundreds or even tens of meters. It is rarely possible to have the same spatial density of observations from a ship.

Field observations alone often lack large-scale view and repeatability. Ice rings and ice metamorphism in the regions of eddies are a surface manifestation of eddies under the ice. In this respect satellite observations is a very effective method to identify ice rings and thus to detect lens-like eddies. This helps to focus field research, as well as to find new eddies. Satellite
465 monitoring provides statistics on the locations, lifetime, and behaviour of ice rings and lens-like eddies.

Further research with the use of multi-satellite imagery, in situ measurements, and numerical and laboratory modelling will bring further information on eddies under ice: their influence on ice cover evolution, their role in horizontal and vertical heat and mass exchange, their impact on chemistry and biology of the lakes and on human activity.

470 **Author contribution**

AVK performed the analysis, visualisation and writing the original draft. All authors contributed to the ideas, investigation and analysis, writing and editing the paper.

Competing interests:

The authors declare that they have no conflict of interest.

475 **Acknowledgements.**

We would like to thank A.I. Beketov (Ust' Barguzin, Russia) for helpful discussions on ice metamorphism. We acknowledge the use of imagery from the NASA Worldview application (<https://worldview.earthdata.nasa.gov>), part of the NASA Earth Observing System Data and Information System (EOSDIS). Sentinel-1 and Sentinel-2 images - Modified Copernicus



480 Sentinel data [2019-2020]/Sentinel Hub. Landsat-8 image courtesy of the U.S. Geological Survey. Jason-3 data were extracted from the geophysical research data records (GDR) distributed by AVISO+ data portal (avisoftp.cnes.fr).

Financial support

This research has been supported by the CNES TOSCA LakeIce, LAKEDDIES and TRISHNA, ESA CCI+ Lakes, CNRS-Russia IRN TTS projects. A.G. Kostianoy was partially supported in the framework of the P.P. Shirshov Institute of Oceanology RAS (Russian Academy of Sciences) budgetary financing (Project N 0128-2021-0002). E. Zakharova was
485 partially supported by the Federal Order № 0147-2019-0001 to Water Problems Institute RAS .

References

- Ashton, George D. "Ice in lakes and rivers". Encyclopedia Britannica, 21 Jun. 2007, <https://www.britannica.com/science/lake-ice>. Accessed 17 March 2021.
- Circles in thin ice, Lake Baikal, Russia. NASA Earth Observatory, Image of the day - 25 May 2009.
490 <http://earthobservatory.nasa.gov/IOTD/view.php?id=38721>. Assessed 17 March 2021.
- Evans C.A., Lulla K.P., Dessinov L.V., Glazovskiy N.F., Kasimov N.S., Knizhnikov Yu.F. Shuttle-Mir Earth Science investigations: Studying Dynamic Earth from the Mir Space Station. In "Dynamic Earth Environments. Remote Sensing observations from Shuttle-Mir Missions, Eds Lulla K.P., Dessinov L.V., Evans C.A., Dickerson P.W. and Robinson J.A. Wiley, 2000, p. 1-14.
- 495 Giant gas bubble found in Lake Baikal may explode at any moment, Moskovskiy Komsomolets, 12 May 2020 (In Russian). <https://www.mk.ru/science/2020/05/12/ogromnyy-gazovyy-puzyr-obnaruzhenny-v-baykale-mozhet-vzorvatsya-v-lyubuyu-minutu.html>, accessed 17 March 2021.
- Granin N.G, Makarov, M.M., Kucher, K.M., Gnatovsky, R.Y. 2008. The deep water gas seeps in Lake Baikal. Proceedings of the 9th International Conference on gas in marine sediments, Bremen, Germany, 15–19 September, p. 76–77.
- 500 Granin, N. G., Mizandrontsev I.B., Kozlov V;V;, Tsvetova E.A., Gnatovskii R.Yu., Blinov V.V., Aslamov I.A., Kucher K.M., Ivanov V.G., Zhdanov A.A. 2018. Natural ring structures on the Baikal ice cover: Analysis of experimental data and mathematical modeling. Russian Geol. Geophys. 59: 1514–1525. doi:<https://doi.org/10.1016/j.rgg.2018.10.011>
- Granin, N. G., V. V. Kozlov, E. A. Tsvetova, and R. Y. Gnatovsky. 2015. Field studies and some results of numerical modeling of a ring structure on Baikal ice. Doklady Earth Sci. 461: 316–320.
- 505 Granin, N.G., Wüest, A., Gnatovskii, R.Yu., Kapitanov, V.V., 2005. Evidence of activity of mud volcanoes in Baikal, in: The Fourth Vereshchagin Baikal Conference: Abstracts of Papers and Posters, 26 September–1 October, 2005 [in Russian]. Institute of Geography SB RAS, Irkutsk, pp. 52–53.



- Kääb A., Altena B., Mascaro J. River-ice and water velocities using the Planet optical cubesat constellation *Hydrol. Earth Syst. Sci.*, 23, 4233–4247, 2019 <https://doi.org/10.5194/hess-23-4233-2019>
- 510 Kostianoy A.G., Belkin I.M. A survey of observations on intrathermocline eddies in the World Ocean. - Proc. 20-th Int. Liege Colloq. Ocean Hydrodyn. "Mesoscale/synoptic coherent structures in geophysical turbulence", J.C.J.Nihoul, B.M.Jamart (Eds.), Amsterdam, Elsevier, 1989, P.821-841.
- Kouraev A.V., Zakharova E.A., Rémy F., Kostianoy A.G., Shimaraev M.N., Hall N.M.J., Suknev A.Ya., Giant ice rings on Lakes Baikal and Hovsgol: inventory, associated water structure and potential formation mechanism, *Limnology and*
- 515 *Oceanography* 61, 2016, p. 1001-1014, doi: 10.1002/lno.10268
- Kouraev A.V., Zakharova E.A., Rémy F., Kostianoy A.G., Shimaraev M.N., Hall N.M.J., Zdrovennov R.E., Suknev A.Ya. Giant ice rings on lakes and field observations of lens-like eddies in the Middle Baikal (2016-2017). *Limnology and Oceanography*, 2019, Vol 64, p. 2738-2754, doi: 10.1002/lno.11338
- Kouraev A.V., Zakharova E.A., Rémy F., Kostianoy A.G., Shimaraev M.N., Hall N.M.J., Suknev A. Ya. Ice cover and water
- 520 dynamics in lakes Baikal and Hovsgol from satellite observations and field studies. In "Remote Sensing of Asian Seas", Editors: V. Barale, M. Gade, Springer, 2018, pp. 541-555
- Kouraev A.V., Zakharova E.A., Rémy F., Suknev A.Ya. Study of Lake Baikal ice cover from radar altimetry and in situ observations. - *Marine Geodesy*, Special issue on SARAL/AltiKa, 38:sup1, 477-486, DOI: 10.1080/01490419.2015.1008155
- 525 Obolkina L.A., Bondarenko N.A., Doroshenko L.F., Gorbunova L.A., Molozhavaya O.A. Discovery of cryophilic community in Lake Baikal. *Doklady of the Russian Academy of Sciences*, 2000, Vol. 371, No 6, p. 815-817 (In Russian).
- Planet Team (2017). Planet Application Program Interface: In Space for Life on Earth. San Francisco, CA. <https://api.planet.com>.
- "Remote Sensing of Earth from space in Russia" - Scientific and practical magazine, Issue No 2, 2020, Roskosmos, p. 14-15.
- 530 Sokol'nikov V.M. Radiation properties of Lake Baikal ice and some events of ice regime in Maloye More. Preceedings of the Baikal Limnological station, USSR Academy of Sciences. 1959, Vol XVII, p. 104-107.
- Zakharova E.A., Agafonova S., Duguay C., Frolova N., Kouraev A.V. River ice phenology and thickness from satellite altimetry. Potential for ice bridge road operation. - *The Cryosphere Discussions*, 2021, submitted.
- Zyryanov V.N., Granin N.G., Zyryanov D.V., Chebanova M.K., Aslamov I.A., Gnatovsky R.Yu., Blinov V.V. "Preliminary
- 535 results of the summer and winter companies 2019-2020 on Lake Baikal in the framework of the RFBR project for the study of eddies that form ice rings". *Limnology and Freshwater Biology* 2020 (4): 954-955. SI: "The VII-th Vereshchagin Baikal Conference" DOI:10.31951/2658-3518-2020-A-4-954